Automation in Construction 165 (2024) 105537

Contents lists available at ScienceDirect

Automation in Construction

journal homepage: www.elsevier.com/locate/autcon

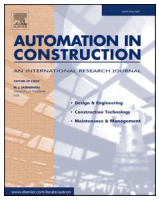

Autoencoder-based Photoplethysmography (PPG) signal reliability enhancement in construction health monitoring

Yogesh Gautam, Houtan Jebelli *

Department Civil and Environmental Engineering, University of Illinois Urbana-Campaign, Champaign, IL, United States of America

ARTICLE INFO

Keywords:
Construction worker health monitoring
Convolutional neural network
Photoplethysmography
Motion artifact
Autoencoder
Anomaly detection

ABSTRACT

Prior research has validated Photoplethysmography (PPG) as a promising biomarker for assessing stress factors in construction workers, including physical fatigue, mental stress, and heat stress. However, the reliability of PPG as a stress biomarker in construction workers is hindered by motion artifacts (MA) - distortions in blood volume pulse measurements caused by sensor movement. This paper develops a deep convolutional autoencoder-based framework, trained to detect and reduce MA in MA-contaminated PPG signals. The framework's performance is evaluated using PPG signals acquired from individuals engaged in specific construction tasks. The results demonstrate the framework has effectiveness in both detecting and reducing MA in PPG signals with a detection accuracy of 93% and improvement in signal-to-noise ratio by over 88%. This research contributes to a more reliable and error-reduced usage of PPG signals for health monitoring in the construction industry.

1. Introduction

Ensuring physical and mental well-being of construction workers has been a persistent and pressing issue. Chronic fatigue is among the primary areas of concern within the construction industry, notably, in the United States, a substantial 40% of construction workers encounter severe fatigue at some stage throughout their workday [1]. Added to the physical health complexities, construction workers are also among the most prone to mental problems [2]. The implementation of continuous health monitoring technology for construction workers holds tremendous potential in addressing these multifaceted challenges.

The significant advancements in the microchip industry witnessed over recent decades have paved the way for the transformation of physiological devices into compact wearable forms. Real-time detection of various stressors relating to physical and mental fatigue/stress from wearable sensors can help inform better decisions regarding health in real-time, which can thus prevent severe fatalities and related health problems [3]. Extensive research has been conducted on various wearable health monitoring devices suitable for implementation in construction sites including electrocardiogram (ECG), electromyography (EMG), and photoplethysmography (PPG) [4–10].

PPG which measures blood volume pulse (BVP) has access to various cardio-pulmonary activities such as blood pressure, oxygen saturation (SpO_2), and pulse rate, providing access to various stressors like physical fatigue, mental stress, and heat stress [11]. In addition, wearable PPG sensors also have the advantages of compact size, ease of use, and lower power usage [12]. However, despite these promising findings, the widespread adoption of photoplethysmography for health monitoring in the construction industry has been relatively limited.

One significant challenge in using wearable PPG sensors for health monitoring is their susceptibility to motion artifacts [13]. Motion artifacts are the distortions in signal waveform arising from bodily movements or external factors leading to inaccurate blood volume measurements. Such distorted signals can undermine the reliability and accuracy of health assessments using PPG signals. This issue is particularly exacerbated when subjects are engaged in various physical activities, intensifying the occurrence of motion artifacts [12–14]. The construction setting, characterized by substantial physical activity, further magnifies the challenge of motion artifacts in acquired signals. Observational data and studies in construction show that tasks with manual labor and tool usage often cause significant hand and body motions [15,16]. Existing literature on ergonomic assessments in construction also demonstrates this, emphasizing the prevalence of hand-intensive tasks like material handling, rebar tying, hammering, drilling, and scaffold erection [17–22]. These activities involve repetitive and intensive hand movements, impacting the accuracy of PPG signals by introducing motion artifacts.

Addressing the challenge of motion artifacts in PPG signals has been

* Corresponding author.
E-mail addresses: ygautam2@illinois.edu (Y. Gautam), hjebelli@illinois.edu (H. Jebelli).

https://doi.org/10.1016/j.autcon.2024.105537
Received 6 September 2023; Received in revised form 3 June 2024; Accepted 5 June 2024
Available online 10 June 2024

the subject of extensive research, leading to the development of two primary approaches for the detection and filtering of MA in PPG signals: acceleration-based methods and non-acceleration-based methods. Acceleration-based methods use motion data based on acceleration as a reference to track device motion and subsequently use this information to reduce motion artifacts [23–26]. While this approach can be leveraged for both tasks of detection and artifact reduction, it has two major drawbacks: (i) requirement of extra hardware and its calibration, and (ii) higher power requirement. While these may not be an issue in a lab setting under a controlled environment, they may pose challenges in real-world application wearable devices that require small size and lower power consumption. Moreover, MA in the acquired PPG signal and acceleration data may not strongly correlate as well [27].

Non-acceleration-based methods may be broadly categorized into feature extraction-based fiducial methods and wavelet transform methods. Fiducial methods rely on waveform features and statistical descriptors of the PPG waveform for the detection of motion artifacts. While these methods are easier to implement, they require manual feature engineering, exhibit relatively lower performance, and encounter challenges when confronted with diverse testing environments [28]. Wavelet transform-based methods eliminate the need for feature engineering, offering both noise reduction and detection capabilities. However, they may introduce phase distortion and loss of data during processing [29].

The limitations associated with these existing methods create a notable knowledge gap, one that could be effectively addressed by leveraging deep learning-based approaches. Deep learning (DL) methods have been able to achieve superior performance for artifact removal in similar physiological signals like EEG [30–33] and ECG [34–36]. Furthermore, DL has also proven to be a powerful tool in various healthcare applications based on PPG signals [37–41]. This paper introduces a novel non-acceleration-based deep learning framework that employs an autoencoder architecture to detect and reduce motion artifacts in PPG signals. An autoencoder is a neural network architecture comprising two primary components: an encoder and a decoder. The encoder transforms input data into a condensed, lower-dimensional representation, extracting essential features. The decoder then reconstructs the input data from this representation, effectively reducing noise and capturing salient patterns. This makes autoencoders particularly effective for tasks like artifact detection and noise removal. Recent studies have underscored the effectiveness of deep autoencoder networks in denoising across diverse domains, including images [42,43], videos [44,45], audio signals [46,47], and physiological signals [30,48].

Building upon the autoencoder architecture, the proposed framework comprises two main components capable of screening and reducing motion artifacts in the input PPG signals. The initial component utilizes the autoencoder network for anomaly detection to detect MA-induced PPG signals. The second component employs the autoencoder network to reconstruct MA-contaminated PPG signals, effectively reducing motion artifacts. The developed framework has been trained and validated using data acquired in a construction environment, featuring subjects engaged in diverse construction tasks such as material handling and rebar tying. This tailored approach enhances the framework's relevance to the construction domain, especially the ones involving hands-on and intensive construction activities. The integration of screening and motion artifact reduction within a unified autoencoder network also improves computational efficiency and memory utilization. Consequently, this study fills a critical gap in current approaches and contributes significantly to the field by presenting a comprehensive framework for motion artifact screening and removal in PPG signals. The ensuing development is positioned to streamline scalable and reliable deployment and expand the applications of health monitoring based on physiological sensing, particularly offering substantial benefits to the construction industry.

The paper is structured as follows: In Section 2, a brief literature review is provided, focusing on health monitoring through photoplethysmography and the existing methods of MA reduction in photoplethysmography signals. Section 3 describes the proposed methodology, including the technical details of the autoencoder-based framework for MA detection and removal. In Section 4, a case study is presented, which includes details of the experiments conducted to develop and evaluate the framework. The results are analyzed and discussed in Sections 5 and 6. Finally, the contributions are summarized in Section 6 and Section 7 concludes the paper.

2. Literature review

2.1. PPG for health monitoring

Photoplethysmography is a non-invasive optical method that measures blood volume changes in peripheral blood vessels [49]. These changes generate pulsating signals captured through PPG, comprising an AC (alternating current) and DC (direct current) component. AC component is primarily induced by blood volume changes with each heartbeat, while the DC component represents baseline tissue absorption. The AC component is essential for deriving pulsatile information, while the DC component is associated with static physiological conditions [50]. PPG sensors have gained widespread acceptance in the field of medicine, serving various purposes, including the assessment of blood oxygen saturation (SPO2), heart rates, and related metrics such as pulse rate, heart rate variability, and blood pressure [51]. The invaluable access to cardio-pulmonary data has made them a common tool for cardiovascular monitoring. In clinical settings, they have proven effective in detecting multiple cardiovascular conditions like arterial stiffness, peripheral artery disease, and hypertension [52,53]. Furthermore, PPG sensors have also been employed for respiratory rate monitoring, identifying sleep apnea, and assessing pain levels [54,55].

The application of photoplethysmography has also been explored for the construction industry [56]. The author's prior research investigated the feasibility of utilizing PPG technology to assess the physical and mental well-being of construction workers [5]. The work was able to verify the statistical dependence of the physical and mental status of a worker to derivatives of PPG like heart rate variation. Numerous studies have been conducted in construction settings to explore the applications of photoplethysmography to assess construction workers' health status. For instance, Shakerian et al. developed a datacentric approach using PPG signals and machine learning algorithms for detecting heat stress among workers in construction sites. The work validated in the construction environment was able to predict distinct levels of heat strains among multiple subjects with the use of PPG signals [4]. In another work, Shayesteh et al. leveraged PPG signals as a part of a multimodal analysis employing convolutional neural networks to determine cognitive loads during construction training tasks performed in a virtual environment [57]. Despite the potential of PPG in accessing various health conditions of workers its usage in real world can be impacted by noise contamination.

2.2. Motion artifact detection and removal in PPG signals

One of the major sources of noise in acquiring PPG signals is the motion artifact [26,58]. Motion artifact in photoplethysmography refers to unwanted variations in the PPG signal caused by movement noise, leading to inaccurate or distorted measurements of blood volume changes. Because of the overlapping of MA frequency and pulsating component of the PPG signal, separation of the MA from the signal using a traditional filter-based-approach is not efficient [59]. PPG signal acquisition relies on the optical reflection and absorption of light in tissues, making it susceptible to distortion with even slight movements, given the rapid nature of this process. In clinical environments with constrained motion, mitigating motion artifact (MA) issues is feasible. However, in realistic operational scenarios where motion is inevitable,

the susceptibility to contamination poses a significant challenge in acquiring high-quality PPG signals [60].

Feature extraction-based fiducial methods have been extensively researched in the literature for artifact detection. One of the approaches is based on waveform feature extraction like peak interval, amplitude, pulse width, etc. based on time and period domain analysis, where MA is detected based on the anomalous waveform features [59,61]. The other type of approach is based on statistical descriptors such as skewness, root-mean-square, kurtosis, etc. [62,63]. While feature-extracting morphology-based methods are easy to implement, require less data, and are limited to detection tasks [29]. Advanced statistical modeling approaches have also been explored in the literature, for instance, Lee et al. used multichannel PPG signals with varying wavelengths applying independent component analysis to reduce MA in the acquired PPG signal [64]. In a separate study, Zhang et al. employed distinct wavelengths for signal acquisition to reduce motion artifacts in PPG. Utilizing one wavelength as a motion reference helped diminish motion artifacts in the acquired PPG signals [65]. While multiple wavelengths and devices can offer an improved performance, the use of multiple sensors can encounter potential hardware configuration challenges and the placement location of the multiple sensors can impact the accuracy and consistency of the results.

Wavelet transform-based techniques have the advantage over the fiducial methods as it doesn't require feature engineering and comparatively provide a superior performance [66–69]. However, wavelet transform-based methods may introduce phase distortion in signals, which can cause a loss of information as well as provide misleading inferences [70]. Another frequently used method involves utilizing IMU, gyroscope, or accelerometers to track device motion and subsequently using this information to detect, estimate, and subsequently remove motion artifact [23–25]. While this approach can be leveraged for both tasks of detection and artifact reduction, it requires extra hardware, and calibration, and has higher power usage. Moreover, motion artifacts in the PPG signal and accelerometer data do not strongly correlate as well [27].

2.3. Autoencoder based artifact removal

Deep learning offers numerous advantages over traditional signal processing methods. It adeptly captures complex relationships facilitating the building of generalizable models. It can automate feature extraction, thus enabling faster systems and end-to-end learning frameworks. These desirable features have established deep learning as a powerful tool for signal processing and denoising tasks [30,31,34,36,39,71,72].

Recent studies have also explored various machine learning-based methods for artifact removal in PPG signal. Zargari et al. developed a non-acceleration method using a combination of Convolutional Neural Network (CNN) and Cycle Generative Adversarial Network (CycleGAN) to detect and remove MA in PPG signals [73]. CNN identifies MA in the first phase, and CycleGAN is then applied in the second phase for artifact reduction. While the model demonstrated improved performance compared to both fiducial and wavelet-based methods, the use of CycleGAN, known for its complex architecture, may bring computational challenges for real-world applications. The need for separate neural network models for detection and reduction, along with the computational cost, can pose difficulties for real-time in-device computation, especially in wearables.

Autoencoders, a class of neural networks, have shown unique promise in addressing the intricacies of motion artifact detection and removal. These networks generally have simpler and smaller architecture compared to advanced models like cycleGAN while can perform well in denoising and generative tasks. Unlike traditional methods that rely on manual feature engineering, autoencoders automate the process of feature extraction, allowing for a more adaptive and nuanced approach to capturing the underlying patterns in PPG signals. Their ability to learn hierarchical representations of data makes them particularly suited for handling the varying morphologies of physiological signals across individuals and environments [30,74].

As efficient as these methods can be such autoencoder models have not been investigated for motion artifact detection and removal for PPG signals. Therefore, this study aims to design, deploy, and validate a novel end-to-end framework based on an autoencoder network for MA detection and removal in PPG signals, specifically tailored to the construction environment. The development of this framework will facilitate scalable deployment and expanded applications of physiological sensing-based health monitoring within the construction industry.

3. Autoencoder network for motion artifact removal

This section describes the different components of the proposed autoencoder-based framework for motion artifact screening and removal. The framework is developed through four primary phases presented in Fig. 1. In the first phase, data acquisition is performed for subjects in a controlled construction setting with prespecified construction tasks for a predetermined time frame. Through the experiment, motion artifact-free reference PPG signals and MA-contaminated PPG signals are acquired for the study. Further details regarding this phase are provided in Section 4. In the second phase, the PPG signals acquired in the first phase are preprocessed to train the autoencoder in the third phase. In this phase, filtering methods are applied to remove workplace-related extrinsic artifacts, and normalizing, windowing methods are used to prepare the signal into a suitable format for training the autoencoder network for the third phase. In the third phase, the preprocessed PPG signal is used to train an autoencoder network that learns to reconstruct the MA-free signal as the output of the network. The autoencoder network developed in the third phase is deployed in the final phase to develop an anomaly detector for detecting and screening MA in the PPG signal. In this phase, the PPG signals with MA are detected and screened based on the reconstruction error of the autoencoder network. So, the developed framework comprises of two dependent systems based on the developed autoencoder network to screen and remove motion artifacts in the acquired PPG signals. For testing the performance of the framework, data acquired from multiple subjects performing construction tasks is leveraged. The second, third, and fourth phases are explained in the following subsections.

3.1. Signal preprocessing

After the PPG signals are acquired in the form of Blood volume Pulse (BVP) from subjects performing specific construction tasks (section: “Experimental Study: PPG Dataset from construction Scenarios”), the signals are preprocessed through four different steps. First, low pass filter of 10 Hz is applied to remove high-frequency extrinsic noise for construction environment corresponding to electrical noises, electromagnetic, and thermal noises [75]. After applying the filter, the signals are normalized by minmax normalization. This normalization ensures that all the values lie between 0 and 1, which complies better with the network architecture training process.

To enhance the autoencoder network's generalizability, the reference PPG signal acquired during the stationary phase is augmented with various types of artificial noise during the training phase. A combination of gaussian noise, Brownian noise, pink noise, blue noise, and violet noise is used to synthesize artificially contaminated PPG signals. This combination has been used based on work [76]. Gaussian noise uses the uniform normal distribution centered around 0. This adds up frequency invariant noise as power spectral density is constant across all the frequencies. Pink noise has a frequency spectrum in which the power spectral density (PSD) of the signal is inversely proportional to the frequency while Brownian noise has a frequency spectrum with the PSD of the signal inversely proportional to the square of frequency. Similarly, violet and blue noise have a frequency spectrum with the PSD of the

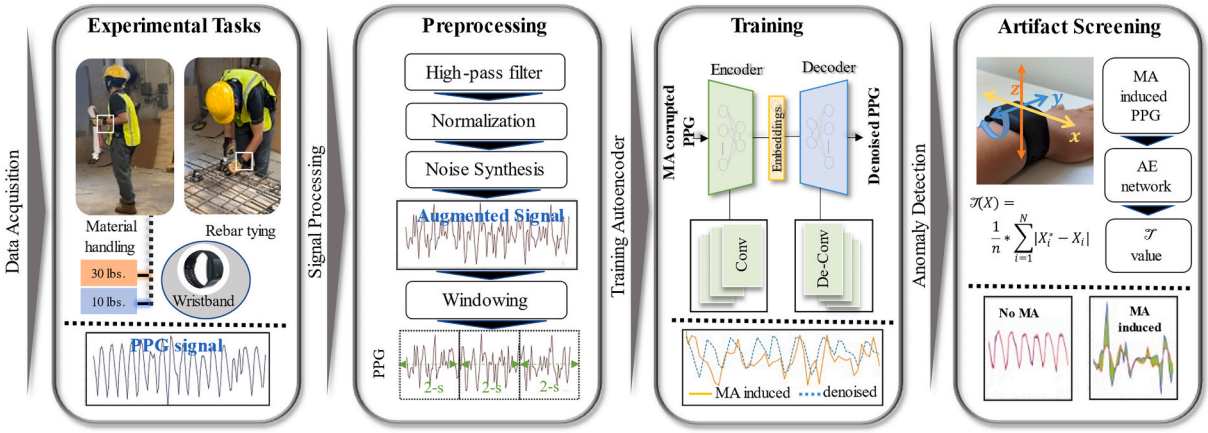

Fig. 1. Overview of the proposed study.

signal directly proportional to the frequency and its square respectively. These contaminated signals are combined with the reference signals to augment the training set. This ensures that the autoencoder learns to reconstruct artifact-reduced PPG signals from multiple variations of the contaminated signal thus increasing the generalizability of the developed system [76].

Windowing is performed after the noise synthesis. Since a neural network can process only a fixed length of temporal data, the network needs to be fed with a batch of fixed-length temporal series during training. For creating the windowed dataset, a sliding window of 2 s time is used with a stride of 2 s. Thus, for a single instance of processing of the autoencoder network, 2 s of PPG signals are reconstructed. A normal healthy human has a pulse rate from 60 to 100 beats per minute which is a periodicity of <1 s, but for diseased cases like bradycardia, it may be lower to around 40–60 bpm. To make the network effective for extreme cases, a larger temporal range of two seconds is used as the input size. This enables the monitoring system to make health inferences based on a single instance of denoised PPG signals. A representation of various forms of augmented noise with sampled windows is presented in Fig. 2.

3.2. Network architecture and training

After performing the required signal processing, the designed autoencoder network is trained. The autoencoder network comprises two parts, an encoder and a decoder connected by an embedding layer, as shown in Fig. 3. The encoder leverages PPG signals from photoplethysmography as input to generate column vector in latent space, $v = \{v_1, v_2, \ldots, v_4\}$, that is used to reconstruct the PPG signals through the decoder subnetwork. The encoder is constructed of two convolutional blocks followed by two dense layers of 16 and 4 units respectively which extract features into the embedding layer. For the first convolution block (C_1), kernel size of 5×1 is used to capture a larger temporal range. This allows the network to learn features over a broader time window. In the second convolution block (C_2), a reduced kernel size of 3×1 is used to capture more detailed and localized features in the PPG signal. For the first and second convolutional blocks, 8 and 16 filter sizes are used respectively. The choice of increasing filter sizes facilitates a hierarchical feature learning approach. Smaller filters in the first block can capture simple, low-level features, while larger filters in the second block can focus on more complex patterns. Each convolutional block consists

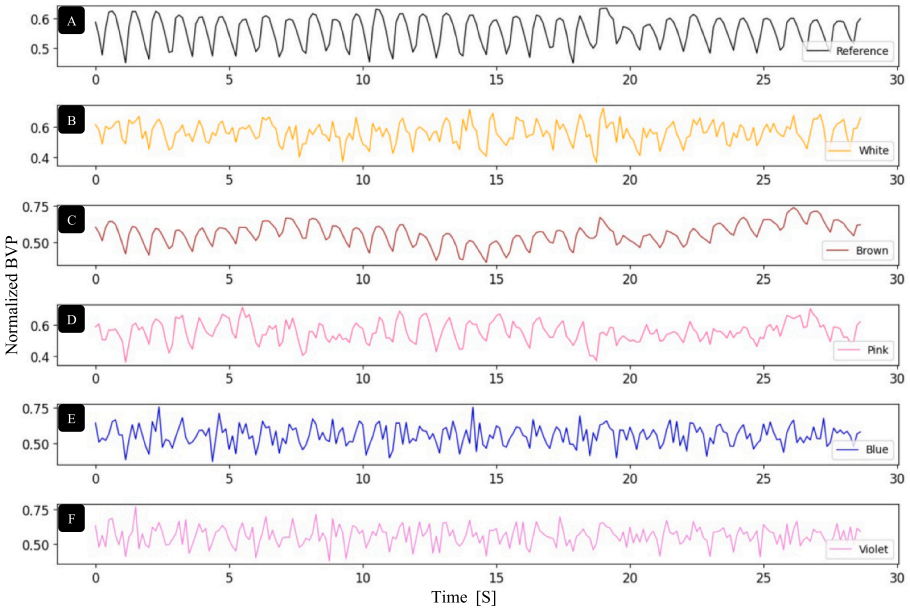

Fig. 2. Sample of augmented signals compared with reference PPG signal. 2 A: Reference PPG signal; Various noise added to the reference signal as follows: 2B: White noise added signal; 2C: Brown noise added signal; 2D: Pink noise added signal; 2E: Blue noise added signal; 2F: Violet noise added signal. (For interpretation of the references to colour in this figure legend, the reader is referred to the web version of this article.)

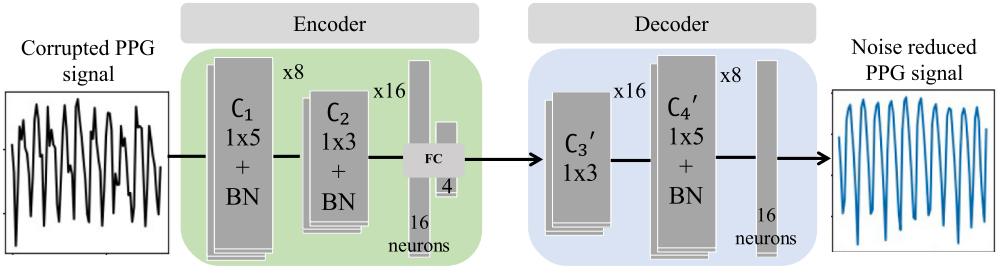

Fig. 3. Architecture of the developed autoencoder network for artifact reduction.

of 1D convolution followed by batch normalization and max pool layer. Batch normalization helps in stabilizing and accelerating the training process by normalizing the input of each layer. Max pool layer is used for down sampling the learned features, thus focusing on the most important feature, and reducing computational load for the network. Two dense layers follow the convolutional blocks with 16 and 4 units, respectively. The reduction in units in the second dense layer is aimed at reducing the dimensionality of the latent space, potentially extracting more salient features for reconstruction. The decoder leverages the output of the encoder, a column vector in latent space, to reconstruct the PPG signals by reducing the artifacts. The decoder is constructed of two transposed convolutional blocks followed by a dense layer, to generate the denoised PPG signals. In the transposed convolutional blocks, a kernel size of 3×1 is used in the first deconvolution layer (C_3'), while a kernel size of 5×1 is chosen in the second deconvolution layer (C_4'). These kernel sizes are selected to reverse the effects of the convolutional layers effectively, allowing the network to learn to denoise the PPG signals. The first deconvolution layer comprises of 16 filters, and the second deconvolution layer comprises of 8 filters. The use of decreasing filter sizes helps the network gradually reconstruct the PPG signals while reducing the complexity of learned features. Each transposed convolutional block consists of 1D deconvolution followed by batch normalization, which is used to stabilize and accelerate the training process by normalizing the input for the next layer. The final dense layer comprises of 16 units pertaining to the final output size of the reconstructed signal, ensuring that the final output size of the reconstructed signal aligns with the input PPG signals.

For the training process, the mean absolute error is used as the loss function $\mathscr{L}(\theta)$ (Eq. (1)). During each iteration, the weight parameters (θ) of the network are updated to θ^* to minimize the given loss function as given by Eq. (1).

$$\Theta^* = \text{argmin}_\theta \left(\sum_i^N \left| f_{re}\left(X_i^*, \theta\right) - X_i \right| \right) \tag{1}$$

The reference signals and the augmented signals acquired during the stationary phase are utilized for training the autoencoder network. Here, X_i^* is the input augmented PPG signal where as X_i is reference motion artifact free PPG signal and the autoencoder reconstructed output $f_{re}\left(X_i^*, \theta\right)$ is the output of the network. Eq. (1) will measure the difference between the reference signal (X_i) and the autoencoder reconstructed signal $f_{re}\left(X_i^*, \theta\right)$ and reduce the mean absolute difference by optimizing weights of the autoencoder network (θ). Through iterating and optimizing value for the weights (θ), the autoencoder network learns to generate the PPG signals without noises. During the training of the autoencoder, the loss function as described in Eq. (1) was minimized using the Adam optimizer [67]. A learning rate of 0.001 was chosen for the training process. The value was determined using a learning rate scheduler where performance was evaluated for varying range of learning rate for $1e-5$ to 0.1. TensorFlow API with Keras backend was used for developing and training the autoencoder network [77]. During the training, a ratio of 80:20 was used for the training and validation set. Moreover, to ensure generalizability during data split, two primary methodologies were leveraged: stratified sampling and the inclusion of a holdout set [78]. Stratification, conducted on a subject-wise basis, ensured that data from all subjects was represented in both the training and test sets, exposing the network to a diverse range of data within the specified set. Additionally, a distinct holdout set was allocated comprising data from ten subjects, enabling the evaluation of the network's performance on unseen data that played no role in the training process. This incorporation of a holdout set served as a crucial measure for assessing the model's efficacy in handling novel and untrained instances.

The performances of the training were evaluated based on Mean absolute error (MAE), Mean squared error (MSE), and Signal-to-noise ratio (SNR) as defined in [79]. For the validation set, improvement SNR as defined by [68] and given in Eq. (2) was used as the evaluation metrics.

$$\Delta\text{SNR} = 10log_{10}\left(\frac{\sigma_{\text{ref}}^2}{\sigma_{\text{denoised}}^2}\right) - 10log_{10}\left(\frac{\sigma_{\text{ref}}^2}{\sigma_{\text{noisy}}^2}\right) \tag{2}$$

$$\gamma = 100\left(1 - \frac{R_{\text{ref}} - R_{\text{denoised}}}{R_{\text{ref}} - R_{\text{noisy}}}\right) \tag{3}$$

Here, $\sigma_{\text{ref}}^2, \sigma_{\text{denoised}}^2$, and σ_{noisy}^2 represents the variance of the MA free reference PPG signal, denoised PPG signal, and contaminated PPG signal respectively. For the reduction in motion artifact (γ) (Eq. (3)), R_{ref}, R_{denoised}, and R_{noisy} represent correlation coefficient for MA free reference signal, denoised signals and noisy signal respectively.

3.3. Motion artifact detection using anomaly detection

An anomaly detection algorithm is further developed by leveraging the trained autoencoder network for screening PPG signals with motion artifacts. A separate set of experiments as described in section 4.2 are performed to examine the performance for four different variations of MA-induced PPG signals. For each MA-inducing activity, acquired PPG signals are fed as the input to the autoencoder, and reconstruction MAE is computed against the PPG signal output by the autoencoder network. The time-averaged reconstruction MAE is leveraged to examine and compare motion artifacts for various MA-inducing activities as given by Eq. (4). The minimum reconstructing MAE value is used as the reference to screen motion artifacts in the acquired PPG signals. For each sequence of PPG signals processed through the autoencoder, the reconstruction MAE is computed using Eq. (4). If the computed value exceeds the reference reconstruction MAE, the signal is flagged as an artifact signal and undergoes the denoising process. Otherwise, it is classified as a no artifact signal, and thus is not processed for the denoising process.

$$T(X) = \frac{1}{n}^* \sum_{i=1}^{N} |y_i - X_i| \tag{4}$$

Here, $T(X)$ represents the reconstruction MAE value for the given sequence of PPG signals, y_i represents the reconstructed PPG signals which is output by the autoencoder network whereas x_i represents the MA induced PPG signals, which is the input for the autoencoder

network. The subscript i represents i^{th} data point in the given sequence of PPG signal.

3.4. Evaluation of individual differences

The acquired PPG signals can have varying morphology across different individuals and construction tasks which can cause variations in the performance of the developed framework. An evaluation method specifically targeting individual differences is set to assess the robustness of the developed framework and validate its performance across individual variations. Recognizing potential variations in PPG signal patterns among participants, a Kullback-Leibler (KL) divergence test [80] was integrated into the evaluation process. The KL divergence test quantifies the information difference between two given distributions. It assesses the dissimilarity between the two distributions P and Q by calculating the sum of the products of the probability of each event in P with the logarithm of the ratio of the probabilities in P and Q (Eq. (5)) [80].

$$D_{KL}\left(P\,||Q\right) = \sum\nolimits_i P(i) log\left(\frac{P(i)}{Q(i)}\right) \tag{5}$$

Here, $D_{KL}(P\,||Q)$ represents the KL divergence values for given distribution P and Q whereas, P and Q represent the distributions of SNR values obtained from the MA-induced and MA-reduced PPG signals respectively. The values obtained from the KL divergence test for these two distributions are then evaluated for the varying tasks and individuals using one-way analysis of variance ANOVA. The one-way ANOVA is a statistical test used to determine whether there are any statistically significant differences between the means of the given groups. Mathematically, it is the ratio of between-group variability and within-group variability as given by Eq. (6).

$$F = \frac{\sum_i n_i(\overline{X}_i - \overline{X})^2 \Big/ (k-1)}{\sum_i \sum_j \left(X_{ij} - \overline{X}_i\right)^2 (N-k)} \tag{6}$$

Here, n is the number of observations in the i^{th} group. Each type of construction task can be considered as a different group to evaluate the variance across varying tasks, $\overline{X}_i$ is the mean of the i^{th} group, $\overline{X}$ is the overall mean, X_{ij} is the j^{th} observation in the i^{th} group, k is the number of group (types of construction tasks) and N is the total number of observation (number of individuals). The parameters and results are presented and discussed in more detail in Section 5.

4. Experimental study: PPG dataset from construction scenarios

To assess the developed framework's performance in screening and removing motion artifacts from PPG signals, a case study was conducted in a construction setting. An off-the-shelf wristband biosensor was used to acquire PPG signals from the subject ("E4 wristband") [81]. In total, 15 subjects were employed for the study providing a relatively diverse sample. The inclusion of multiple individuals helps capture a range of physiological variations that may be present in PPG signals. The data collection was performed in two sets of distinct phases: the stationary phase and the construction phase. Data acquired during the stationary phase was used as a reference signal during training and data acquired during the specific construction task was used for evaluating the developed framework. In total four construction tasks were performed, three construction tasks were performed in a real environment whereas, for the fourth task, virtual reality (VR) was used where subjects performed material handling task in a high-rise building designed in virtual environment. As the sensor used in the study is wristband type device, the experimental construction tasks had been carefully selected to ensure their common occurrence in the construction workplace as well as involve significant hand or upper body motion. Three specific material handling tasks were selected for the study, given that manual material handling stands out as one of the most prevalent activities in construction, demanding substantial hand and body motions [22]. Additionally, manual rebar tying, another common construction task, also involving significant hand movements was also chosen for the experimental tasks [82]. The chosen tasks are not only widely encountered in the construction environment but also exhibit significant motion, ensuring the relevance of the experiments to both the construction setting and the MA reduction framework. Additionally, the VR based material handling task was included to add diversity to the acquired PPG signals by introducing a more immersive and potentially stressful construction environment for the subjects. The inclusion of various tasks aimed to capture different stressors and physical activities that might affect the morphology of the PPG signals differently across individuals. Across the subjects, the mean age, weight, and height were 24.6 years, 182 pounds and 5′11″ respectively with a standard deviation of 3.5 years, 14 pounds and 5″ respectively. The experiments are illustrated in Fig. 4.

4.1. Data acquisition for training and evaluation of the autoencoder network

For every subject, initially, PPG signals were acquired for the stationary phase which is leveraged as the motion artifact-free reference signal for training the autoencoder network. The subjects were seated comfortably and asked to rest their hand on a table in a stationary position and the PPG signal was acquired. In case the subjects wished to move or take a break, the signals acquisition was temporarily halted and then resumed once the subject was ready. For each subject, PPG signals were acquired for one hour in the stationary phase. 10% of the data acquired during the stationary experiment is allocated for testing the screening system. For further examining the developed framework for the construction environment, PPG signals were acquired in construction settings where the subjects performed various construction related tasks like material handling and rebar tying. Data from ten subjects is used as holdout set for evaluation of the framework in construction environment. Four different tasks were performed in the construction environment, which mainly comprised of material handling and rebar tying, which are among the most common manual tasks in construction [22]. The diversity in tasks aimed to cover a spectrum of motion artifacts that might be induced by different hand and body movements. The first task was a rebar-tying task. In this task, the subjects tied up rebars set up in an area of 1.21 m by 0.6 m for a total of 20 min with a small voluntary break if required by the subject. The subjects use manual wire twister to tie up the rebar with a wire tie. The second task was a low-intensity material handling task where subjects transported a load of 2.3 Kg (5 lbs.) within a distance of 6 m. This task was performed for around 15 min with a short voluntary break if required by the subject. The third task was high-intensity material handling, for which the same setup as that of material handling task was used but with a load of weight 13.6 Kg (30 lbs.). The fourth task was performed in a virtual environment, subjects were asked to carry a lightweight interactable load between two given locations at 6 m distance in the virtual environment. In the virtual environment, the subjects were working in a high-rise building steel structure lacking fences and a concrete base. This task was performed to acquire signals from subjects in a more realistic construction setting without compromising the safety of the subject. Subjects reporting or doubtful of acrophobia were excluded from this experiment as the virtual environment is set up at a significant height and open environment. For the construction setting, thus 3.456 million instances of data points of PPG signal were available for developing and examining the autoencoder-based framework.

4.2. Experiment to set threshold values for MA detection

To develop and assess the performance of the MA screening

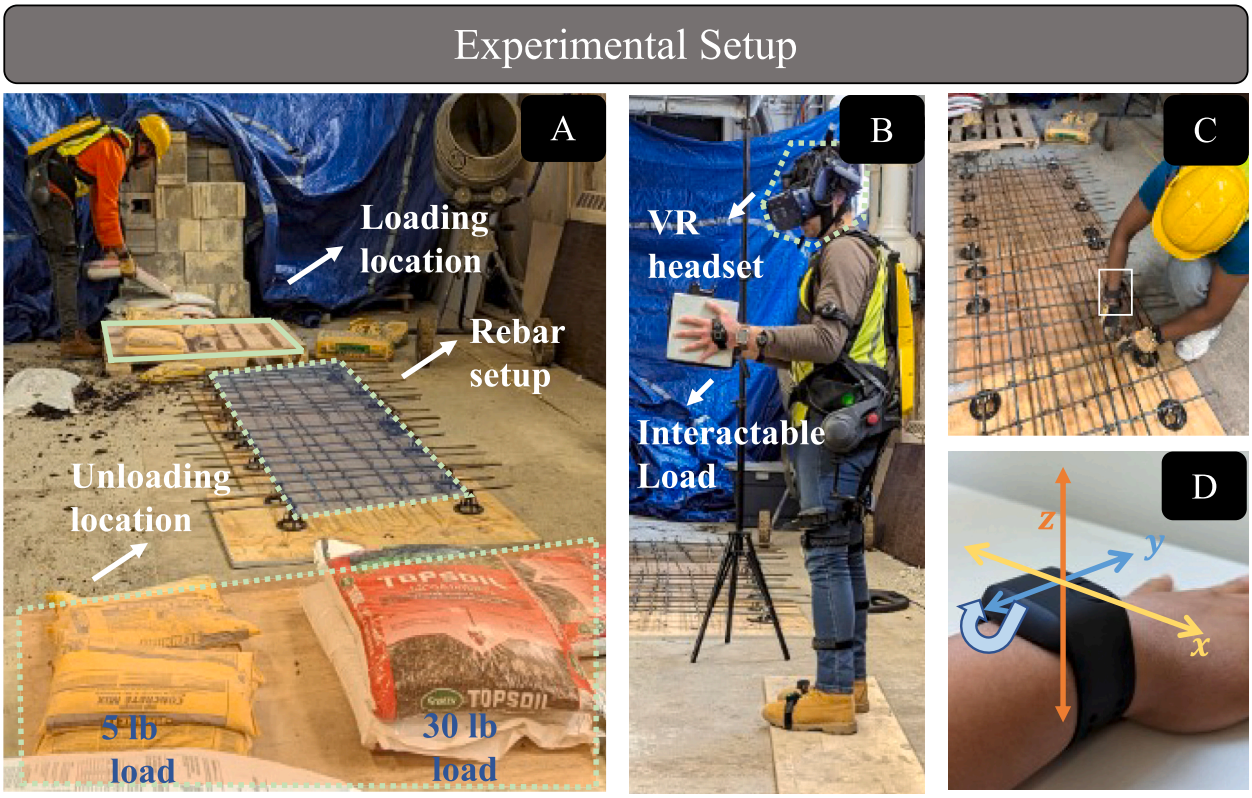

Fig. 4. Experimental setup and tasks for the case study; 4 A: Experimental setup for the construction tasks and a subject performing material handling task; 4B: Subject performing material handling task in a virtual environment with the interactable load; 4C: Subject performing rebar tying task with the wristband bounded in white outlined box; 4D: A coordinate system for the wristband used in this study.

component of the developed framework, the authors conducted a separate set of tasks to acquire MA-induced PPG signals. In this experiment, MA-induced PPG signals were acquired from subjects by inducing various forms of hand motion of the subject. The experimental protocol is designed based on the work of [83], where various amplitude and frequencies of vertical head motion were induced for subjects in a controlled environment during EEG signal acquisition for studying various forms of motion artifacts in EEG signal. Since similar experimental protocols were not available in the literature for studying MA in PPG signals, the experimental design drew inspiration from the previously mentioned investigation.

The experiments aimed to obtain MA-induced PPG signals through controlled hand motion for the wristband type PPG sensor. The direction of motion for the x, y, and z axes was defined relative to the device coordinate system, as depicted in Fig. 4D. To simulate hand motion, the wristband was subjected to periodic, forceful displacement of 10 mm in the x-direction for a duration of 60 s during PPG signal acquisition from the subject's wrist. The same procedure was implemented to induce y-motion and z-motion, wherein the wristband underwent forceful displacement in the y-axis and z-axis directions with an amplitude of 10 mm, respectively. In the fourth task, the wristband was worn with a loose fit with a circumferential clearance of 2 mm and 4 mm. Two sets of experiments were performed at these two levels. Random hand waving task was performed during the experiments to generate MA-induced PPG signals. In total, the fourth task was performed for about 6 min, as signals acquired during this task were also leveraged to test the MA detection algorithm.

For testing the accuracy of the motion detection algorithm, stationary phase and MA-induced PPG signals were combined in equal proportions. For stationary signals, signals acquired in section 4.1 are leveraged whereas for MA-induced PPG signals, data acquired during the loose-fit task explained in the previous paragraph is leveraged.

5. Results

This section presents the results of training and testing the autoencoder-based framework for MA detection and reduction. For MA reduction, the performances were evaluated based on Mean absolute error (MAE), Mean squared error (MSE), and Signal-to-noise ratio (SNR) [73]. A further evaluation of the performance of the denoising method was performed on signals acquired from the construction tasks as explained in Section 4.1. For evaluating the performance of the high MA screening component, reconstruction MAE as given by Eq. (4) was used as the evaluating metric, and data acquired during tasks explained in section 4.2 was leveraged.

5.1. MA removal using autoencoder

For the development of the framework, the autoencoder network was trained as explained in Section 3. During the training of the autoencoder, the loss function as described in Eq. (1) was minimized using the Adam optimizer [77]. TensorFlow API with Keras backend was used for designing and developing the autoencoder network [78]. For training and validation purposes, MSE, SNR and improvement SNR as described in Section 4.1 was leveraged. A sample of denoised PPG signal compared with the contaminated signals is presented in Fig. 5.

For computing reduction in motion artifact (γ) (Eq. (3)), the MA induced and the denoised PPG signals' correlation coefficient is measured against the MA free reference signal. Also, the correlation coefficient for the reference signal (R_{ref}) is set to 1 as the R_{ref} is used as the reference for calculating the correlation coefficient for the given equation. During the training of the autoencoder network, for the training and the validation set, improvement SNR were 2.01 and 1.90 respectively, whereas the reduction in motion artifact was 10.94% and 3.7% respectively.

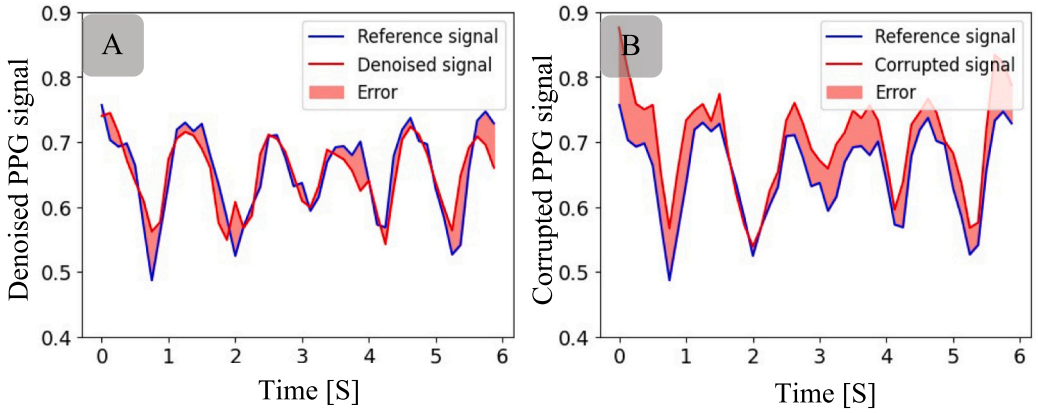

Fig. 5. Sample output for the denoised signal from the test set; A: Autoencoder output of the denoised PPG signal compared with the reference signal; B: Contaminated PPG signals compared with the reference PPG signal.

For further testing the performance of the developed autoencoder for the construction environment, PPG signals acquired from subjects performing construction tasks as defined in Section 4.1 were leveraged. The contaminated SNR was computed for the unprocessed PPG signals acquired during the construction task whereas the denoised SNR was computed for the MA removed signals reconstructed by the autoencoder network. The subject-wise calculation for SNR values for various construction tasks is presented in Fig. 6.

Upon evaluation of subject-wise SNR values, Rebar tying tasks have a comparatively lower initial SNR which may be attributed to the fact that rebar tying involves continuous motion of hand in jerky manner which can induce comparatively more MA than material handling tasks which involves only limited hand motion during loading and unloading activities. Also, it is observed that subject 9 has a consistently high SNR value for all three real construction tasks compared to other subjects (Fig. 6). This may be caused by personal working style with limited or controlled hand motion which could have induced less MA in the acquired PPG signals. As expected, M3, or the material handling task performed in VR has the highest SNR values both for MA contaminated and denoised signals. The VR material handling didn't involve loading and unloading tasks, the subjects were walking between the given points in the virtual construction environment transporting the load with minimal movement of the hand because of which MA corruption in the signal could have been lower thus resulting in higher SNR values. In average rebar tying task had an increase in SNR by 90% whereas the VR based material handling it was only 59%. In average, the initial SNR values for the raw PPG signals acquired had a SNR value of 9.579 whereas the average SNR value for the MA reduced PPG signal was 18.05, thus providing an increase in the SNR values by 88%.

5.2. *MA detection and thresholding using the autoencoder network*

The reconstruction MAE values obtained for the previously defined MA-inducing tasks are presented in Table 1. The threshold values along x, y, and z directions were comparatively higher as in these cases MA was induced by direct forceful movement of the device along the wrist to

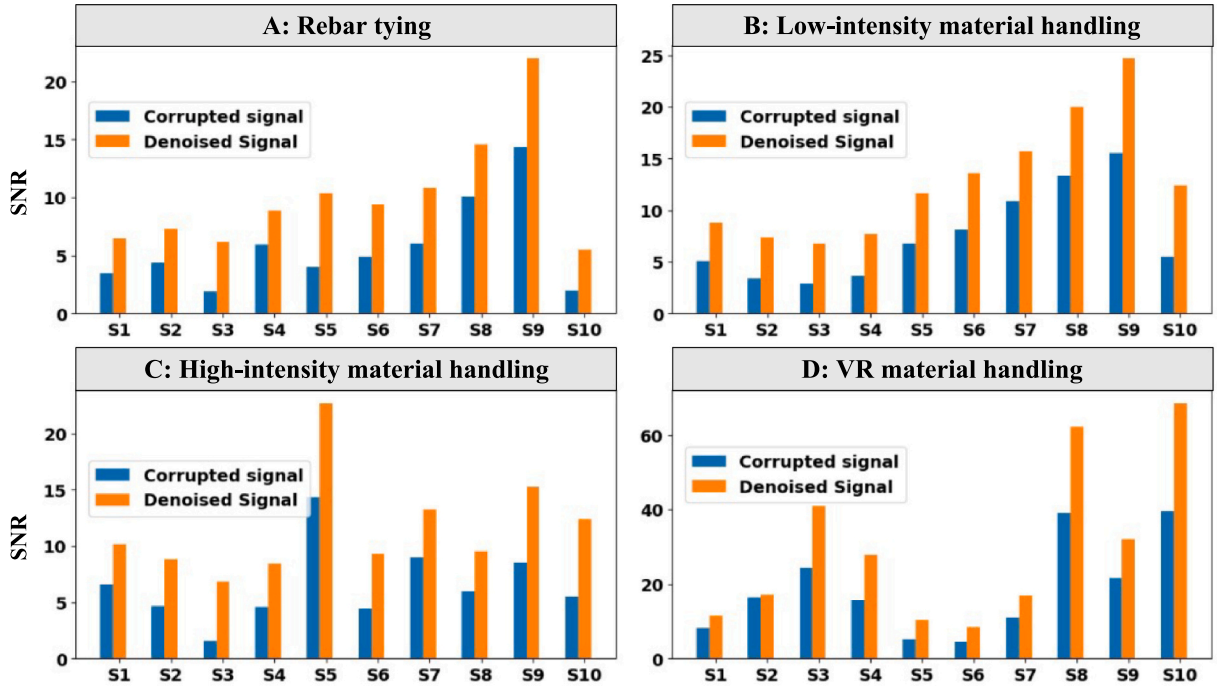

Fig. 6. Subject-wise SNR values for various construction tasks; 6 A: SNR value for Low-intensity material handling; 6B: SNR value for high-intensity material handling; 6C: SNR value for VR material handling.

Table 1
Threshold values for various types of MA introduced in the study.

S.no.	Type of MA induced	MAE reconstruction	MSE threshold
1	X-motion	0.242	0.119
2	Y-motion	0.244	0.094
3	Z-motion	0.094	0.014
5	Loose fit - random motion	0.0405	0.108

a specified amplitude of 10 mm. For the loose fit random motion, the natural movement of the device was leveraged without directly applying displacement to the device along the wrist. A sample of reconstruction for all the experiments is presented in Fig. 7. As the loose fit-random motion resembled more to natural hand motion like waving its reconstruction error was used as the reference threshold value for the autoencoder-based anomaly detector. Thus, a reconstruction error of 0.0405 was set as the threshold value for detecting MA-induced PPG signals. The sample of detected MA signals is presented in Fig. 8.

The algorithm was further tested on a test set comprising of signals acquired during loose fit-random motion and stationary phase data acquisition as described in Section 4.2 and Section 4.1 respectively. The algorithm has an accuracy of 93% with a precision of 95% and a recall of 90%. In this scenario, prioritizing higher precision is paramount. By doing so, the screening process for MA induced PPG signals is enhanced, ensuring a more accurate filtering mechanism. This, in turn, prevents the erroneous inclusion of MA induced PPG signals in the health monitoring system, thereby reducing the risk of incorrect health inferences.

The performance of the developed framework was further evaluated to validate variations in response to individual differences. To address potential individual variations in PPG signal patterns and ensure the generalizability of test results, a Kullback-Leibler (KL) divergence test was employed. The KL divergence quantified the variance in signal-to-noise ratio distributions in the PPG signals with and without motion artifacts i.e., the MA induced input signal and MA reduced output signal. This value was computed for every individual (10 individual) in the test set across every experimental task (3 material handling and 1 rebar tying). The test allowed for a nuanced examination of how the proposed MA removal technique was performed across diverse individuals and conditions. The values obtained from the KL divergence test were compared for individuals using one-way ANOVA to analyze differences across individuals. The test yielded values as follows: an f-statistic of 0.89 and a *p*-value of 0.46. The f-statistic value of 0.89, closer to 1, indicated that the differences between individuals were not much larger than the differences within individuals (inter-variability within various tasks for a given individual). As the p-value of 0.46 is >0.05, it suggests that any observed differences between the individuals could be due to random variability rather than variability between the groups. This indicates there were no significant differences between the performance of the framework for different individuals. Not having significant differences between individuals suggests an effective generalization of the proposed framework.

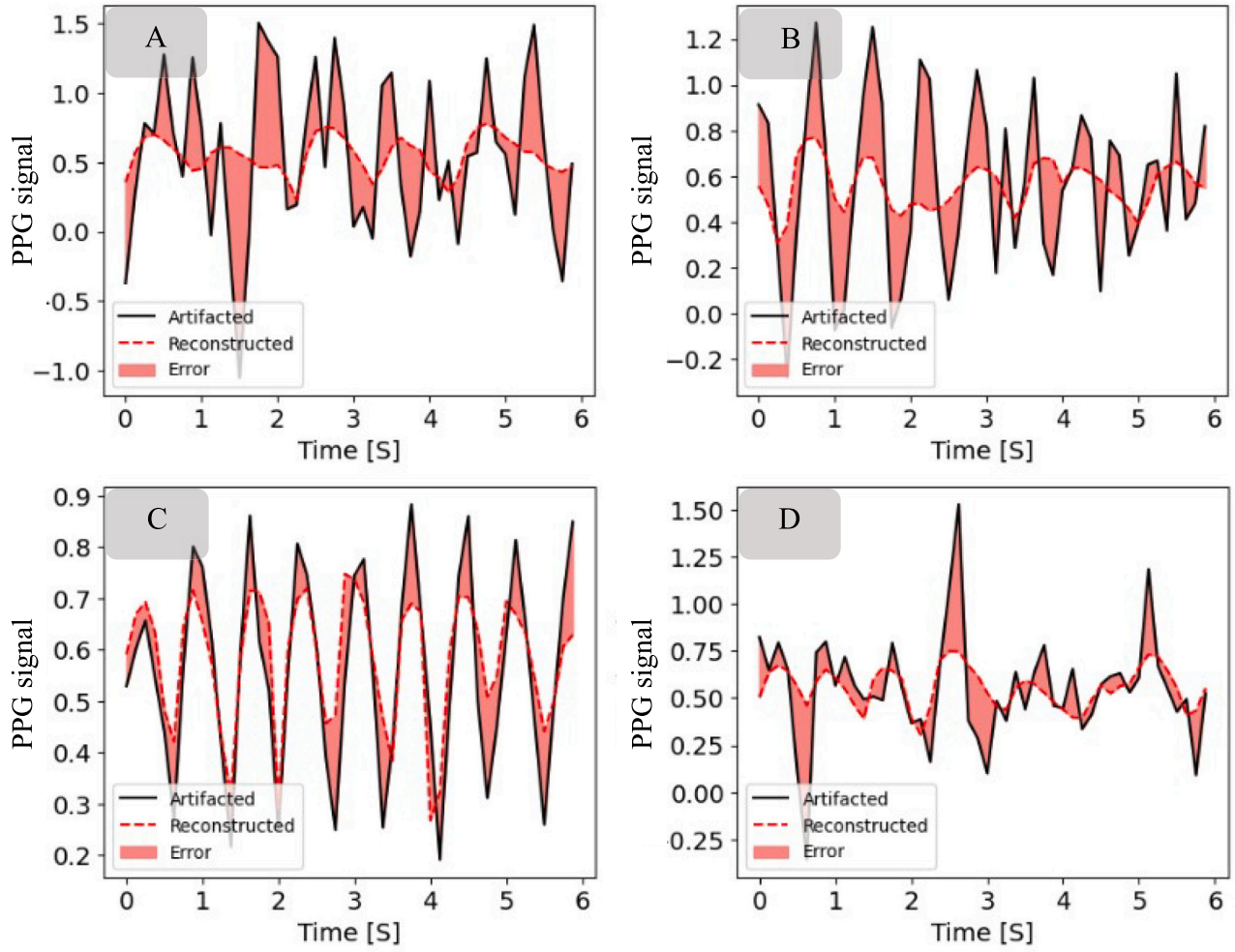

Fig. 7. Sample of MA-induced signals and corresponding reconstructed signals; 6 A: X-axis MA-induced PPG signal; 6B: Y-axis MA-induced PPG signal; 6C: *Z*-axis MA-induced PPG signal; 6D: Loose fit MA-induced PPG signal.

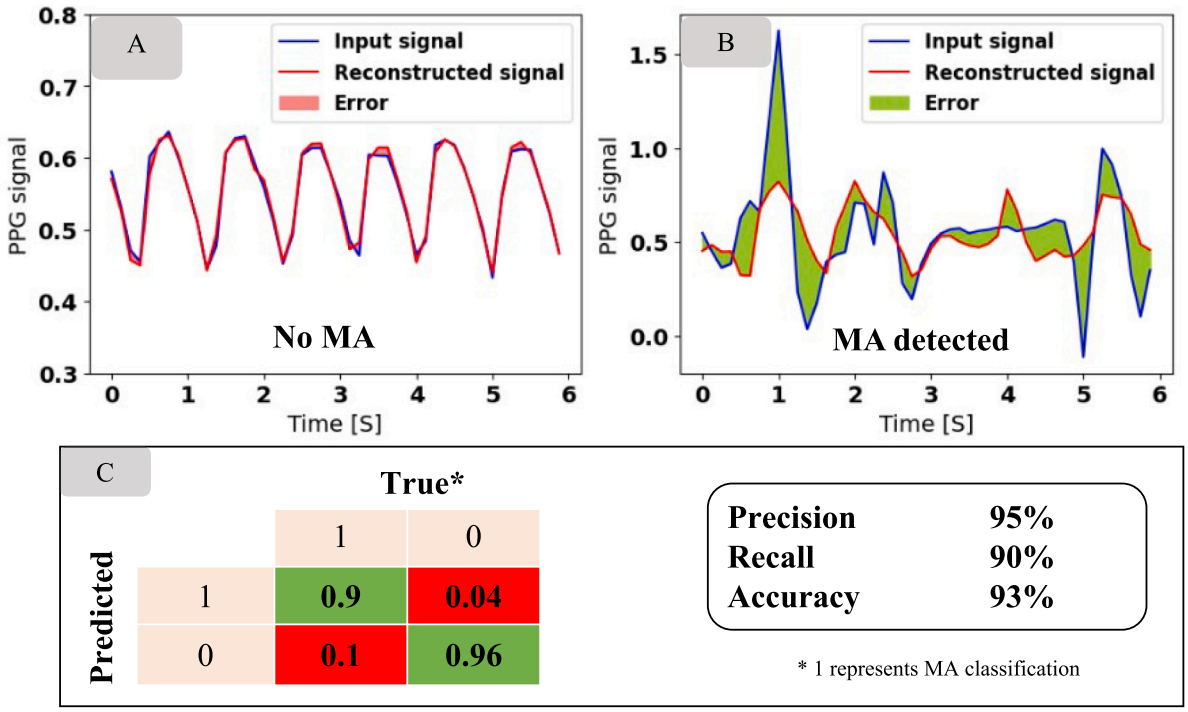

Fig. 8. MA detector results on test set; A: No MA classification; B: MA induced signal classification; C: Normalized confusion matrix for the test set with key metrics.

6. Discussion

The proposed autoencoder-based framework demonstrated its efficacy in screening and reducing motion artifacts in PPG signals acquired during intense and dynamic activities such as construction tasks. For signals acquired during construction tasks, the framework was able to provide improvement in SNR by over 88% and detect high MA PPG signals with an accuracy of 93%. The authors also compared the performance of this framework with that of existing non-acceleration-based motion artifacts detection and removal approaches which have comprehensively been evaluated by literature and have approved performance, these were mainly chosen based on literature review comparing performance metrics. A separate comparison was performed for MA detection and MA reduction. For MA reduction, the compared methods are namely (1) Wavelet decomposition method, (2) Statistical Evaluation, and (3) Interval dependent denoising based on wavelet decomposition [68,84,85]. The results for are presented in Fig. 9. The proposed method provides a 27% higher increase in SNR compared to the competing best method of Interval Dependent denoising.

Similarly, for the comparison of the MA detection function following methods were used leveraged: (1) Gramian Angular Field and 2D CNN, (2) 1D CNN, (3) Adaptive Template Matching, and (4) Random Distortion Testing. The comparison has been summarized in Table 2. Notably, two methods demonstrated comparable detection accuracy to the

Table 2
MA detection performance comparison with other works.

Study	Method	Accuracy (%)
Our study	Autoencoder based reconstruction	93
[86]	Gramian angular field and 2D CNN	94.3
[29]	1D CNN	94.5
[87]	Adaptive template matching	91.5
[88]	Random distortion testing	83

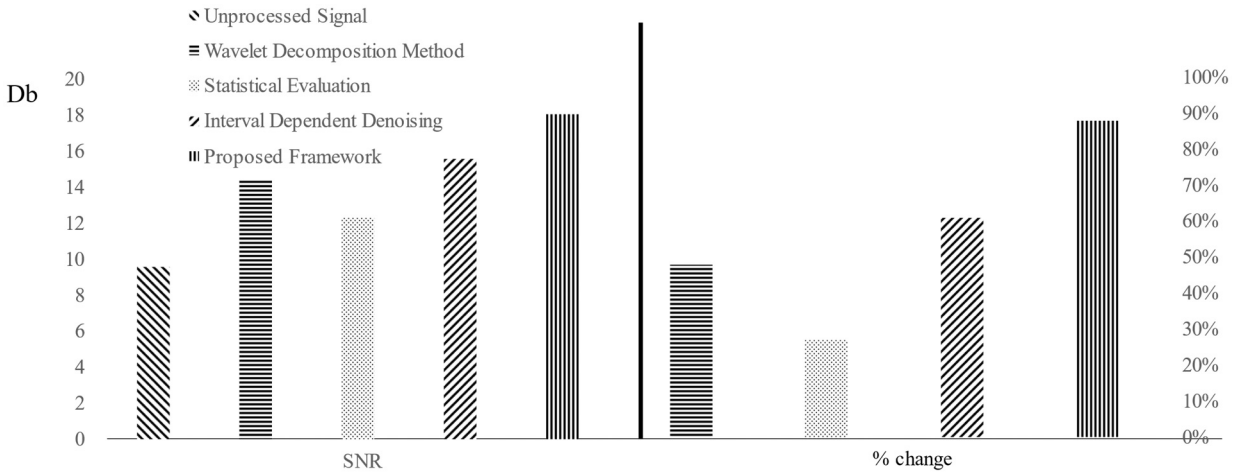

Fig. 9. Comparison of the proposed autoencoder with other denoising methods.

proposed method [29,86]. However, it's important to highlight that these methods comprised of detection systems only and did not incorporate any denoising functionality for the MA-induced PPG signal.

Another important finding was revealed by evaluating the PPG signals acquired during construction activities with the MA detection component of the developed framework. The task-wise classification for instances of signals having MA as a percentage is presented in Table 3. When tested for construction tasks, rebar tying had the highest instances of MA. This may be attributed to the fact that rebar tying involves continuous motion of the hand in a jerky manner which can induce comparatively more MA than material handling tasks which involve only limited hand motion during loading and unloading activities. For the low-intensity and high-intensity material handling, instances of motion artifact fluctuated significantly from subject to subject i.e. for around half of the subject percentage of high MA was higher for task M1 whereas the opposite is for the remaining half. This variation may be because of the variation of load handling behavior of subjects for various loads. As expected, M3, or the material handling task performed in VR had the lowest instances of high MA and almost 0 for most subjects. The VR material handling didn't involve loading and unloading tasks, the subjects were walking between the given points in the virtual construction environment transporting the load with minimal movement of the hand because of which MA instances may be comparatively lower in this task.

The framework was also applied to access motion artifacts in various common construction tasks, distinguishing between hands-on activities, prone to frequent body motion, and supervisory roles, which are generally less physically intensive. Within hands-on activities, MA instances were evaluated for material lifting, hammering, and drilling, while supervisory roles were assessed for walking and computer browsing. The comparative analysis is summarized in Table 4. Tasks involving intensive hand motion, such as hammering and drilling, exhibited a notable incidence of MA. Conversely, less intensive supervisory activities, like walking and computer browsing, showed relatively lower instances of MA. This observation is consistent with the experimental results, where tasks featuring vigorous hand movements tended to have a higher occurrence of motion artifacts. In contrast, activities with lower manual intensity, exemplified by supervisory roles, demonstrated comparatively fewer instances of motion artifacts. This trend aligns with the experimental tasks, where hands-on activities like rebar tying, characterized by intense hand motions, showed a higher frequency of motion artifacts. In contrast, less intensive activities like VR-based material handling, devoid of lifting or intense physical activity, displayed fewer instances of motion artifacts. Understanding these dynamics contributes valuable insights for optimizing MA reduction strategies in construction environments, emphasizing the need for tailored approaches based on the nature and intensity of the tasks involved.

According to the above discussion, the proposed autoencoder-based framework has the potential to promote more efficient health monitoring in the construction industry for construction workers. The framework enables a more reliable usage of PPG signals for various types of cardio-pulmonary monitoring of construction workers both on and off the field in real time. Furthermore, the framework can be integrated into algorithms for detecting various cardio-pulmonary health situations like hypertension, heat stroke, heart attack, etc. This can lead to improved health and quality of life for construction workers, which in turn may also increase overall productivity in construction.

Table 4
Instances of motion artifacts detected (in percentage) for other common construction tasks.

S.no	Tasks	Instances of MA (%)
1	Material Lifting	47.3
2	Hammering	58.2
3	Drilling	52.5
4	Walking	6.2
5	Computer Browsing	15.5

Future research should focus on addressing the various limitations that are still present in this study. Firstly, the accuracy of the MA reduction and detection framework may be negatively impacted by the presence of externalities during signal acquisition sites like dust and sweat which are common in a construction setting. These externalities can be very difficult to tackle as they can completely block any usable signals from being acquired. For instance, the presence of sweat in the wrist may occlude the photoreceptor or the emitter surface which may distort the acquired signals to be unusable for any inference. To overcome this challenge, developments may be necessary for material and hardware design to avoid sweat in the photoreceptors/emitters or use other alternatives for photon-based signal acquisition. Secondly, the current framework mainly focuses on reconstruction errors to detect the high-motion artifact signals and leverages the autoencoder network trained to reduce the noise. To further improve the efficiency of the detection algorithm, the framework can be enhanced by integrating a dedicated ML-based network to detect and classify levels of MA using other variables like wrist acceleration. To this end, one potential avenue for future research is to develop more robust frameworks to tackle problems in construction sites like sweat and dust corruption of the PPG sensors.

7. Contribution

The scientific contribution of this study is highlighted by the introduction of an innovative framework for PPG artifact removal tailored to the construction environment. Through the development of a deep convolutional autoencoder-based framework, the study has achieved a substantial advancement in the accuracy and reliability of PPG signals for health monitoring applications. The proposed framework presents 93% detection accuracy for motion artifacts and a notable improvement of over 88% in the SNR. In contrast to conventional methods that often rely on external hardware or manual feature engineering, the proposed deep learning approach autonomously identifies and rectifies motion artifacts, a critical feature in the dynamic and physically demanding environment of construction sites where traditional methods may prove insufficient.

The technical contributions of the study are underscored by the development of a unified autoencoder framework. This framework can simultaneously detect and reduce MA in PPG signals, simplifying the processing pipeline, and significantly enhancing overall system efficiency in terms of computation and memory usage. The dual functionality within a single framework marks a significant advantage for PPG signal processing. Furthermore, the framework has undergone testing in construction settings, ensuring its practical applicability and

Table 3
Instances of motion artifacts detected (in percentage) for the construction tasks. R1: Rebar tying task; M1: Low-intensity material handling; M2: High-intensity material handling; M3: VR material handling.

Tasks	S1	S2	S3	S4	S5	S6	S7	S8	S9	S10
R1	30.5	10	41.7	3.3	10	13.3	8.3	1.7	19.3	56.3
M1	10.2	18.3	31.7	20.0	8.3	3.3	0.0	0.0	9.2	8.3
M2	8.6	15	21.7	10.0	7.0	18.3	0.0	3.3	7.0	8.3
M3	1.7	0.0	0.0	0.0	5.2	8.0	0.0	0.0	2.5	0.0

effectiveness. Tailored to address the specific needs and challenges of the construction industry, including the high occurrence of motion artifacts due to physical activities, the solution emerges as a relevant and impactful tool for continuous health monitoring of construction workers.

In a broader context, the implementation of this framework has the potential to enhance health monitoring practices in the construction industry. With enhanced accuracy and reliability in detecting stress factors including physical fatigue and mental stress, through PPG signals, the approach can lead to more informed and timely interventions. This will ultimately contribute to the reduction of stress and fatigue-related incidents and improving overall worker well-being. Beyond the construction industry, this research sets a new standard for physiological monitoring in various settings. The principles and methodologies developed here can be adapted and applied to other fields where reliable and efficient health monitoring is crucial, potentially influencing a wide range of health-related practices and technologies.

8. Conclusions

This paper presents a framework to screen and reduce motion artifacts in photoplethysmography signals using a deep autoencoder. An autoencoder network for removing motion artifacts in PPG signals was developed. The developed autoencoder network was further extended to detect and screen MA in the acquired PPG signals. The effectiveness of the developed framework for MA screening and removal was evaluated using PPG signals acquired from human subjects working in a controlled construction environment. The results demonstrated successful implementation of the developed framework with a detection accuracy of 93% and SNR improvement of 88%. The framework developed and evaluated using data acquired in a construction setting, is tailored for the construction environment specially for hands-on and intensive construction activities. The employment of an autoencoder-based MA screening and removal framework can set up the stage for a more reliable health monitoring system for construction workers using PPG signals. The study's findings are relevant for improving the reliability of PPG signals in the health monitoring of construction workers. The proposed framework has the potential to facilitate the digital transformation of health monitoring in construction sites by allowing for accurate and dependable utilization of physiological signals acquired from wearable sensors.

The study has its limitations with real-time deployment as the framework was developed and evaluated on prerecorded data acquired in a controlled construction setting. Real-time deployment may have constraints from existing computation resources in terms of time and memory. In this regard, future research can focus on the real-time deployment of such a framework, optimizing for operational factors like model size, speed, and latency. Another limitation of the proposed framework lies in its susceptibility to external factors, such as dust and sweat, commonly encountered in construction settings. The presence of these externalities can obstruct signal acquisition, particularly when sweat interferes with photoreceptors or emitter surfaces, distorting signals and rendering them unusable for accurate inference. Overcoming this challenge requires innovations in material and hardware design, aiming to either prevent sweat from affecting photoreceptors/emitters or explore alternative methods for photon-based signal acquisition. Furthermore, future investigations can investigate the performance of such frameworks by integrating them to real-time health monitoring systems for better evaluation. It is also recommended to examine other efficient learning models for removing noise like the diffusion models which may provide even better performance. The study successfully implemented the developed framework to address motion artifacts in PPG signals during material handling and rebar tying tasks, including evaluation for individual differences. However, for broader applicability to similar construction tasks, additional validation from future studies may be required to ensure the framework's effectiveness. Similarly, future research could explore the efficacy of the proposed autoencoder-based methods on analogous physiological signals from sources like ECG, EMG, and EEG, which have been utilized in construction health monitoring literature. This could help broaden the scope of applicability of the developed framework.

CRediT authorship contribution statement

Yogesh Gautam: Writing – review & editing, Writing – original draft, Visualization, Software, Methodology, Investigation, Formal analysis, Data curation. **Houtan Jebelli:** Writing – review & editing, Supervision, Resources, Project administration, Methodology, Funding acquisition, Conceptualization.

Declaration of competing interest

The authors declare the following financial interests/personal relationships which may be considered as potential competing interests:

Houtan Jebelli reports financial support was provided by National Science Foundation. Houtan Jebelli reports financial support was provided by National Institute for Occupational Safety and Health. If there are other authors, they declare that they have no known competing financial interests or personal relationships that could have appeared to influence the work reported in this paper.

Data availability

Data will be made available on request.

Acknowledgment

The work presented in this paper was supported financially by a National Science Foundation Award (No. 2401745, 'Future of Construction Workplace Health Monitoring'), and National Institute of Occupational Health and Safety (NIOSH) Grant (No. 1 R21 OH012220-01A1). Any opinions, findings, conclusions, or recommendations expressed in this paper are those of the authors and do not necessarily reflect the views of the National Science Foundation.

References

[1] D. Pablo Ruiz Padillo, J. Antonio Holgado-Terriza, M. Dolores Martínez Aires, S. Sagar Bangaru, C. Wang, F. Aghazadeh, Automated and continuous fatigue monitoring in construction workers using forearm EMG and IMU wearable sensors and recurrent neural network, Sensors 22 (2022) 9729, https://doi.org/10.3390/S22249729.

[2] M.-Y. Leung, Q. Liang, P. Olomolaiye, Impact of job stressors and stress on the safety behavior and accidents of construction workers, J. Manag. Eng. 32 (2015) 04015019, https://doi.org/10.1061/(ASCE)ME.1943-5479.0000373.

[3] S. Hwang, S.H. Lee, Wristband-type wearable health devices to measure construction workers' physical demands, Autom. Constr. 83 (2017) 330–340, https://doi.org/10.1016/J.AUTCON.2017.06.003.

[4] S. Shakerian, M. Habibnezhad, A. Ojha, G. Lee, Y. Liu, H. Jebelli, S.H. Lee, Assessing occupational risk of heat stress at construction: a worker-centric wearable sensor-based approach, Saf. Sci. 142 (2021) 105395, https://doi.org/10.1016/J.SSCI.2021.105395.

[5] H. Jebelli, B. Choi, H. Kim, S. Lee, Feasibility study of a wristband-type wearable sensor to understand construction workers' physical and mental status, in: Construction Research Congress 2018: Construction Information Technology - Selected Papers from the Construction Research Congress 2018 2018-April, 2018, pp. 367–377, https://doi.org/10.1061/9780784481264.036.

[6] A. Ojha, S. Shakerian, M. Habibnezhad, H. Jebelli, Feasibility verification of multimodal wearable sensing system for holistic health monitoring of construction workers, Lecture Notes Civil Eng. 239 (2023) 283–294, https://doi.org/10.1007/978-981-19-0503-2_23/FIGURES/3.

[7] Y. Gautam, Y. Liu, H. Jebelli, Unsupervised adversarial domain adaptation in wearable physiological sensing for construction Workers' health monitoring using Photoplethysmography, construction research congress 2024, CRC 2024 (1) (2024) 339–348, https://doi.org/10.1061/9780784485262.035.

[8] A. Ojha, A. Sharifironizi, Y. Liu, H. Jebelli, Enhancing human-centric physiological data-driven heat stress assessment in construction through a transfer learning-based approach, construction research congress 2024, CRC 2024 (1) (2024) 157–167, https://doi.org/10.1061/9780784485262.017.

[9] S. Shayesteh, A. Ojha, H. Jebelli, Workers' Trust in collaborative construction robots: EEG-based trust recognition in an immersive environment, in: Automation and Robotics in the Architecture, Engineering, and Construction Industry, 2022, pp. 201–215, https://doi.org/10.1007/978-3-030-77163-8_10.
[10] S. Shayesteh, H. Jebelli, Evaluating the feasibility of personalized health status feedback to enhance worker safety and well-being at construction jobsites, construction research congress 2024, CRC 2024 (4) (2024) 575–585, https://doi.org/10.1061/9780784485293.058.
[11] J. Park, H.S. Seok, S.S. Kim, H. Shin, Photoplethysmogram analysis and applications: an integrative review, Front. Physiol. 12 (2022) 2511, https://doi.org/10.3389/FPHYS.2021.808451/BIBTEX.
[12] D. Castaneda, A. Esparza, M. Ghamari, C. Soltanpur, H. Nazeran, A review on wearable photoplethysmography sensors and their potential future applications in health care, Int. J. Biosens. Bioelectroni.cs 4 (2018) 195, https://doi.org/10.15406/IJBSBE.2018.04.00125.
[13] D. Dao, S.M.A. Salehizadeh, Y. Noh, J.W. Chong, C.H. Cho, D. McManus, C. E. Darling, Y. Mendelson, K.H. Chon, A robust motion artifact detection algorithm for accurate detection of heart rates from Photoplethysmographic signals using time-frequency spectral features, IEEE J. Biomed. Health Inform. 21 (2017) 1242–1253, https://doi.org/10.1109/JBHI.2016.2612059.
[14] J. Azar, A. Makhoul, R. Couturier, J. Demerjian, Deep recurrent neural network-based autoencoder for photoplethysmogram artifacts filtering, Comput. Electr. Eng. 92 (2021) 107065, https://doi.org/10.1016/J.COMPELECENG.2021.107065.
[15] J.W. Kim, A. Golabchi, S.U. Han, D.E. Lee, Manual operation simulation using motion-time analysis toward labor productivity estimation: a case study of concrete pouring operations, Autom. Constr. 126 (2021) 103669, https://doi.org/10.1016/J.AUTCON.2021.103669.
[16] V. Paquet, L. Punnett, B. Buchholz, An evaluation of manual materials handling in highway construction work, Int. J. Ind. Ergon. 24 (1999) 431–444, https://doi.org/10.1016/S0169-8141(99)00009-8.
[17] M. Barjasteh, Ergonomic methods to improve safety in the construction sector and reduce costs, Dept. of Indus. and Manuf. Eng., California Polytechnic State Uni., San Luis Obispo, CA, 2010. B.S. thesis, https://digitalcommons.calpoly.edu/imesp/28 (accessed November 18, 2023).
[18] S.D. Choi, L. Hudson, P. Kangas, B. Jungen, J. Maple, C. Bowen, Occupational ergonomic issues in highway construction surveyed in Wisconsin, United States, Ind. Health 45 (2007) 487–493, https://doi.org/10.2486/INDHEALTH.45.487.
[19] A. Ahankoob, A. Charehzehi, Mitigating ergonomic injuries in construction industry, IOSR J. Mechan. Civil Eng. 6 (2024) 36–42, https://doi.org/10.9790/1684-0623642.
[20] M.J.M. Hoozemans, A.J. Van Der Beek, M.H.W. Frings-Dresen, H.F. Van Der Molen, Evaluation of methods to assess push/pull forces in a construction task, Appl. Ergon. 32 (2001) 509–516, https://doi.org/10.1016/S0003-6870(01)00021-7.
[21] M.P. de Looze, T. Bosch, F. Krause, K.S. Stadler, L.W. O'Sullivan, Exoskeletons for industrial application and their potential effects on physical work load, Ergonomics 59 (2016) 671–681, https://doi.org/10.1080/00140139.2015.1081988.
[22] R. Azevedo, C. Martins, J.C. Teixeira, M. Barroso, Obstacle clearance while performing manual material handling tasks in construction sites, Saf. Sci. 62 (2014) 205–213, https://doi.org/10.1016/J.SSCI.2013.08.016.
[23] H.H. Asada, H.H. Jiang, P. Gibbs, Active noise cancellation using MEMS accelerometers for motion-tolerant wearable bio-sensors, in: Annual International Conference of the IEEE Engineering in Medicine and Biology - Proceedings 26 III, 2004, pp. 2157–2160, https://doi.org/10.1109/IEMBS.2004.1403631.
[24] L.B. Wood, H.H. Asada, Noise cancellation model validation for reduced motion artifact wearable PPG sensors using MEMS accelerometers, in: Annual International Conference of the IEEE Engineering in Medicine and Biology - Proceedings, 2006, pp. 3525–3528, https://doi.org/10.1109/IEMBS.2006.260359.
[25] H. Lee, H. Chung, J. Lee, Motion artifact cancellation in wearable Photoplethysmography using gyroscope, IEEE Sensors J. 19 (2019) 1166–1175, https://doi.org/10.1109/JSEN.2018.2879970.
[26] D. Pollreisz, N. TaheriNejad, Detection and removal of motion artifacts in PPG signals, Mobile Netw. Appl. 27 (2022) 728–738, https://doi.org/10.1007/S11036-019-01323-6/TABLES/1.
[27] R. Yousefi, M. Nourani, I. Panahi, Adaptive cancellation of motion artifact in wearable biosensors, in: Proceedings of the Annual International Conference of the IEEE Engineering in Medicine and Biology Society, EMBS, 2012, pp. 2004–2008, https://doi.org/10.1109/EMBC.2012.6346350.
[28] J.W. Chong, D.K. Dao, S.M.A. Salehizadeh, D.D. McManus, C.E. Darling, K.H. Chon, Y. Mendelson, Photoplethysmograph signal reconstruction based on a novel hybrid motion artifact detection–reduction approach. Part I: Motion and noise artifact detection, Ann. Biomed. Eng. 42 (2014) 2238–2250, https://doi.org/10.1007/S10439-014-1080-Y/METRICS.
[29] C.H. Goh, L.K. Tan, N.H. Lovell, S.C. Ng, M.P. Tan, E. Lim, Robust PPG motion artifact detection using a 1-D convolution neural network, Comput. Methods Prog. Biomed. 196 (2020) 105596, https://doi.org/10.1016/J.CMPB.2020.105596.
[30] N.M.N. Leite, E.T. Pereira, E.C. Gurjão, L.R. Veloso, Deep convolutional autoencoder for EEG noise filtering, in: Proceedings - 2018 IEEE International Conference on Bioinformatics and Biomedicine, BIBM 2018, 2019, pp. 2605–2612, https://doi.org/10.1109/BIBM.2018.8621080.
[31] B. Yang, K. Duan, C. Fan, C. Hu, J. Wang, Automatic ocular artifacts removal in EEG using deep learning, Biomed. Sign. Proc. Control 43 (2018) 148–158, https://doi.org/10.1016/J.BSPC.2018.02.021.
[32] S.S. Lee, K. Lee, G. Kang, EEG artifact removal by bayesian deep learning ICA, in: Proceedings of the Annual International Conference of the IEEE Engineering in Medicine and Biology Society, EMBS 2020-July, 2020, pp. 932–935, https://doi.org/10.1109/EMBC44109.2020.9175785.
[33] N. Mashhadi, A.Z. Khuzani, M. Heidari, D. Khaledyan, Deep learning denoising for EOG artifacts removal from EEG signals, in: 2020 IEEE Global Humanitarian Technology Conference, GHTC 2020, 2020, https://doi.org/10.1109/GHTC46280.2020.9342884.
[34] C.T.C. Arsene, R. Hankins, H. Yin, Deep learning models for denoising ECG signals, in: European Signal Processing Conference 2019-September, 2019, https://doi.org/10.23919/EUSIPCO.2019.8902833.
[35] M. Zubair, G.N.V.S. Chandra Mouli, R.A. Shaik, Removal of motion artifacts from ECG signals by combination of recurrent neural networks and deep neural networks, in: ICECIE 2020–2020 2nd International Conference on Electrical, Control and Instrumentation Engineering, Proceedings, 2020, https://doi.org/10.1109/ICECIE50279.2020.9309609.
[36] Y.S. Jhang, S.T. Wang, M.H. Sheu, S.H. Wang, S.C. Lai, Integration design of portable ECG signal acquisition with deep-learning based electrode motion artifact removal on an embedded system, IEEE Access 10 (2022) 57555–57564, https://doi.org/10.1109/ACCESS.2022.3178847.
[37] L. Everson, D. Biswas, M. Panwar, D. Rodopoulos, A. Acharyya, C.H. Kim, C. Van Hoof, M. Konijnenburg, N. Van Helleputte, BiometricNet: Deep Learning Based Biometric Identification Using Wrist-Worn PPG, Proceedings - IEEE International Symposium on Circuits and Systems 2018-May, 2018, https://doi.org/10.1109/ISCAS.2018.8350983.
[38] D. Biswas, L. Everson, M. Liu, M. Panwar, B.E. Verhoef, S. Patki, C.H. Kim, A. Acharyya, C. Van Hoof, M. Konijnenburg, N. Van Helleputte, CorNET: deep learning framework for PPG-based heart rate estimation and biometric identification in ambulant environment, IEEE Trans. Biomed. Circuits Syst. 13 (2019) 282–291, https://doi.org/10.1109/TBCAS.2019.2892297.
[39] X. Chang, G. Li, G. Xing, K. Zhu, L. Tu, DeepHeart, ACM Transactions on Sensor Networks (TOSN) 17, 2021, p. 14, https://doi.org/10.1145/3441626.
[40] M. Panwar, A. Gautam, D. Biswas, A. Acharyya, PP-net: a deep learning framework for PPG-based blood pressure and heart rate estimation, IEEE Sensors J. 20 (2020) 10000–10011, https://doi.org/10.1109/JSEN.2020.2990864.
[41] F. Esgalhado, B. Fernandes, V. Vassilenko, A. Batista, S. Russo, The application of deep learning algorithms for PPG signal processing and classification, Computers 10 (2021) 158, https://doi.org/10.3390/COMPUTERS10120158.
[42] L. Gondara, Medical image denoising using convolutional denoising autoencoders, in: IEEE International Conference on Data Mining Workshops, ICDMW, 2016, pp. 241–246, https://doi.org/10.1109/ICDMW.2016.0041.
[43] X. Ye, L. Wang, H. Xing, L. Huang, Denoising hybrid noises in image with stacked autoencoder, in: 2015 IEEE International Conference on Information and Automation, ICIA 2015 - In Conjunction with 2015 IEEE International Conference on Automation and Logistics, 2015, pp. 2720–2724, https://doi.org/10.1109/ICINFA.2015.7279746.
[44] M.F. Che Aminudin, S.A. Suandi, Video surveillance image enhancement via a convolutional neural network and stacked denoising autoencoder, Neural Comput. & Applic. 34 (2022) 3079–3095, https://doi.org/10.1007/S00521-021-06551-0/FIGURES/9.
[45] J. García-González, J.M. Ortiz-de-Lazcano-Lobato, R.M. Luque-Baena, M. A. Molina-Cabello, E. López-Rubio, Foreground detection by probabilistic modeling of the features discovered by stacked denoising autoencoders in noisy video sequences, Pattern Recogn. Lett. 125 (2019) 481–487, https://doi.org/10.1016/J.PATREC.2019.06.006.
[46] M. Zhao, D. Wang, Z. Zhang, X. Zhang, Music removal by convolutional denoising autoencoder in speech recognition, in: 2015 Asia-Pacific Signal and Information Processing Association Annual Summit and Conference, APSIPA ASC 2015, 2016, pp. 338–341, https://doi.org/10.1109/APSIPA.2015.7415289.
[47] O. Plchot, L. Burget, H. Aronowitz, P. Matějka, Audio enhancing with DNN autoencoder for speaker recognition, in: ICASSP, IEEE International Conference on Acoustics, Speech and Signal Processing - Proceedings 2016-May, 2016, pp. 5090–5094, https://doi.org/10.1109/ICASSP.2016.7472647.
[48] P. Xiong, H. Wang, M. Liu, S. Zhou, Z. Hou, X. Liu, ECG signal enhancement based on improved denoising auto-encoder, Eng. Appl. Artif. Intell. 52 (2016) 194–202, https://doi.org/10.1016/J.ENGAPPAI.2016.02.015.
[49] A.A. Alian, K.H. Shelley, Photoplethysmography, Best Pract. Res. Clin. Anaesthesiol. 28 (2014) 395–406, https://doi.org/10.1016/J.BPA.2014.08.006.
[50] F. Marefat, R. Erfani, P. Mohseni, A 1-V 8.1-μ W PPG-recording front-end with > 92-dB DR using light-to-digital conversion with signal-aware DC subtraction and ambient light removal, IEEE Solid-State Circuits Lett. 3 (2020) 17–20, https://doi.org/10.1109/LSSC.2019.2957261.
[51] T. Arakawa, Recent research and developing trends of wearable sensors for detecting blood pressure, Sensors 18 (2018) 2772, https://doi.org/10.3390/S18092772.
[52] M. Elgendi, R. Fletcher, Y. Liang, N. Howard, N.H. Lovell, D. Abbott, K. Lim, R. Ward, The use of photoplethysmography for assessing hypertension, NPJ Digit. Med. 2 (2019) 1–11, https://doi.org/10.1038/s41746-019-0136-7.
[53] S.M. Zekavat, K. Aragam, C. Emdin, A.V. Khera, D. Klarin, H. Zhao, P. Natarajan, Genetic Association of Finger Photoplethysmography-Derived Arterial Stiffness Index with blood pressure and coronary artery disease, Arterioscler. Thromb. Vasc. Biol. 39 (2019) 1253–1261, https://doi.org/10.1161/ATVBAHA.119.312626.
[54] G.R. Ashisha, X. Anitha Mary, Advances in photoplethysmogram and electrocardiogram signal analysis for wearable applications, Adv. Intellig. Syst. Comp. 1167 (2021) 527–534, https://doi.org/10.1007/978-981-15-5285-4_52/FIGURES/3.
[55] M. Radha, P. Fonseca, A. Moreau, M. Ross, A. Cerny, P. Anderer, X. Long, R. M. Aarts, A deep transfer learning approach for wearable sleep stage classification with photoplethysmography, NPJ Digit. Med. 4:1 (2021) 1–11, https://doi.org/10.1038/s41746-021-00510-8.

[56] Y. Liu, A. Ojha, H. Jebelli, H. Cheng, Enhancing Human-Centric Physiological Data-Driven Heat Stress Assessment in Construction through a Transfer Learning-Based Approach, 2024 Construction Research Congress (CRC), 2024.
[57] S. Shayesteh, A. Ojha, Y. Liu, H. Jebelli, Human-robot teaming in construction: evaluative safety training through the integration of immersive technologies and wearable physiological sensing, Saf. Sci. 159 (2023) 106019, https://doi.org/10.1016/J.SSCI.2022.106019.
[58] Y. Liu, Y. Gautam, S. Shayesteh, H. Jebelli, M. Mahdi Khalili, Towards an efficient physiological-based worker health monitoring system in construction: an adaptive filtering method for removing motion Artifacts in physiological signals of workers, in: Computing in Civil Engineering 2023: Resilience, Safety, and Sustainability - Selected Papers from the ASCE International Conference on Computing in Civil Engineering 2023, 2024, pp. 483–491, https://doi.org/10.1061/9780784485248.058.
[59] R. Couceiro, P. Carvalho, R.P. Paiva, J. Henriques, J. Muehlsteff, Detection of motion artifact patterns in photoplethysmographic signals based on time and period domain analysis, Physiol. Meas. 35 (2014) 2369, https://doi.org/10.1088/0967-3334/35/12/2369.
[60] Y.K. Lee, O.W. Kwon, H.S. Shin, J. Jo, Y. Lee, Noise reduction of PPG signals using a particle filter for robust emotion recognition, in: Digest of Technical Papers - IEEE International Conference on Consumer Electronics, 2011, pp. 202–205, https://doi.org/10.1109/ICCE-BERLIN.2011.6031807.
[61] P.K. Lim, S.C. Ng, N.H. Lovell, Y.P. Yu, M.P. Tan, D. McCombie, E. Lim, S. J. Redmond, Adaptive template matching of photoplethysmogram pulses to detect motion artefact, Physiol. Meas. 39 (2018) 105005, https://doi.org/10.1088/1361-6579/AADF1E.
[62] N. Selvaraj, Y. Mendelson, K.H. Shelley, D.G. Silverman, K.H. Chon, Statistical approach for the detection of motion/noise artifacts in Photoplethysmogram, in: Proceedings of the Annual International Conference of the IEEE Engineering in Medicine and Biology Society, EMBS, 2011, pp. 4972–4975, https://doi.org/10.1109/IEMBS.2011.6091232.
[63] R. Krishnan, B. Natarajan, S. Warren, Analysis and detection of motion artifact in photoplethysmographic data using higher order statistics, in: ICASSP, IEEE International Conference on Acoustics, Speech and Signal Processing - Proceedings, 2008, pp. 613–616, https://doi.org/10.1109/ICASSP.2008.4517684.
[64] J. Lee, M. Kim, H.K. Park, I.Y. Kim, Motion artifact reduction in wearable photoplethysmography based on multi-channel sensors with multiple wavelengths, Sensors 20 (2020) 1493, https://doi.org/10.3390/S20051493.
[65] Y. Zhang, S. Song, R. Vullings, D. Biswas, N. Simões-Capela, N. Van Helleputte, C. Van Hoof, W. Groenendaal, et al., Sensors (Basel, Switzerland) 19 (2019), https://doi.org/10.3390/S19030673.
[66] M. Raghuram, K.V. Madhav, E.H. Krishna, N.R. Komalla, K. Sivani, K.A. Reddy, Dual-tree complex wavelet transform for motion artifact reduction of PPG signals, in: MeMeA 2012–2012 IEEE Symposium on Medical Measurements and Applications, Proceedings, 2012, pp. 39–42, https://doi.org/10.1109/MEMEA.2012.6226643.
[67] C.M. Lee, Y.T. Zhang, Reduction of motion artefacts from photoplethysmographic recordings using a wavelet denoising approach, in: APBME 2003 - IEEE EMBS Asian-Pacific Conference on Biomedical Engineering 2003, 2003, pp. 194–195, https://doi.org/10.1109/APBME.2003.1302650.
[68] G. Joseph, A. Joseph, G. Titus, R.M. Thomas, D. Jose, Photoplethysmogram (PPG) Signal Analysis and Wavelet de-Noising, 2014 Annual International Conference on Emerging Research Areas: Magnetics, Machines and Drives, AICERA/ICMMD 2014 - Proceedings, 2014, https://doi.org/10.1109/AICERA.2014.6908199.
[69] K.R. Arunkumar, M. Bhaskar, CASINOR: combination of adaptive filters using single noise reference signal for heart rate estimation from PPG signals, SIViP 14 (2020) 1507–1515, https://doi.org/10.1007/S11760-020-01692-6/FIGURES/6.
[70] C.H. Goh, L.K. Tan, N.H. Lovell, S.C. Ng, M.P. Tan, E. Lim, Robust PPG motion artifact detection using a 1-D convolution neural network, Comput. Methods Prog. Biomed. 196 (2020) 105596, https://doi.org/10.1016/J.CMPB.2020.105596.
[71] H. Purwins, B. Li, T. Virtanen, J. Schlüter, S.Y. Chang, T. Sainath, Deep learning for audio signal processing, IEEE J. Select. Top. Signal. Proc. 13 (2019) 206–219, https://doi.org/10.1109/JSTSP.2019.2908700.
[72] K. Antczak, Deep recurrent neural networks for ECG signal denoising, arXiv preprint arXiv:1807.11551 (2018). https://arxiv.org/abs/1807.11551.
[73] A.H. Afandizadeh Zargari, S.A.H. Aqajari, H. Khodabandeh, A. Rahmani, F. Kurdahi, An accurate non-accelerometer-based PPG motion artifact removal technique using CycleGAN, ACM Trans. Comp. Healthcare 4 (2023), https://doi.org/10.1145/3563949.
[74] P. Xiong, H. Wang, M. Liu, X. Liu, Denoising autoencoder for eletrocardiogram signal enhancement, J. Med. Imag. Health Inform. 5 (2015) 1804–1810, https://doi.org/10.1166/JMIHI.2015.1649.
[75] W. Waugh, J. Allen, J. Wightman, A.J. Sims, T.A.W. Beale, Novel signal noise reduction method through cluster analysis, applied to Photoplethysmography, Comput. Math. Methods Med. 2018 (2018), https://doi.org/10.1155/2018/6812404.
[76] J. Azar, A. Makhoul, R. Couturier, J. Demerjian, Deep recurrent neural network-based autoencoder for photoplethysmogram artifacts filtering, Comput. Electr. Eng. 92 (2021) 107065, https://doi.org/10.1016/J.COMPELECENG.2021.107065.
[77] Keras: Deep Learning for humans. https://keras.io/, 2024 (accessed November 15, 2023).
[78] V.L. Parsons, Stratified Sampling, Wiley StatsRef: Statistics Reference Online, 2017, pp. 1–11, https://doi.org/10.1002/9781118445112.STAT05999.PUB2.
[79] A. Gonzalez-Moreno, S. Aurtenetxe, M.E. Lopez-Garcia, F. del Pozo, F. Maestu, A. Nevado, Signal-to-noise ratio of the MEG signal after preprocessing, J. Neurosci. Methods 222 (2014) 56–61, https://doi.org/10.1016/J.JNEUMETH.2013.10.019.
[80] S. Kullback, Information Theory and Statistics, Dover Publications, 1968.
[81] E4 Wristband, Real-time physiological signals | Wearable PPG, EDA, Temperature, Motion sensors, 2024. https://www.empatica.com/research/e4/ (accessed March 25, 2023).
[82] J.T. Albers, S.D. Hudock, Biomechanical assessment of three rebar tying techniques, Int. J. Occup. Saf. Ergon. 13 (2007) 279–289, https://doi.org/10.1080/10803548.2007.11076728.
[83] A.S. Oliveira, B.R. Schlink, W.D. Hairston, P. König, D.P. Ferris, Induction and separation of motion artifacts in EEG data using a mobile phantom head device, J. Neural Eng. 13 (2016) 036014, https://doi.org/10.1088/1741-2560/13/3/036014.
[84] W. Chen, N. Jaques, S. Taylor, A. Sano, S. Fedor, R.W. Picard, Wavelet-based motion artifact removal for electrodermal activity, in: Proceedings of the Annual International Conference of the IEEE Engineering in Medicine and Biology Society, EMBS 2015-November, 2015, pp. 6223–6226, https://doi.org/10.1109/EMBC.2015.7319814.
[85] S. Hanyu, C. Xiaohui, Motion artifact detection and reduction in PPG signals based on statistics analysis, in: Proceedings of the 29th Chinese Control and Decision Conference, CCDC 2017, 2017, pp. 3114–3119, https://doi.org/10.1109/CCDC.2017.7979043.
[86] X. Liu, Q. Hu, H. Yuan, C. Yang, Motion artifact detection in PPG signals based on Gramian angular field and 2-D-CNN, in: Proceedings - 2020 13th International Congress on Image and Signal Processing, BioMedical Engineering and Informatics, CISP-BMEI 2020, 2020, pp. 743–747, https://doi.org/10.1109/CISP-BMEI51763.2020.9263630.
[87] P.K. Lim, S.C. Ng, N.H. Lovell, Y.P. Yu, M.P. Tan, D. McCombie, E. Lim, S. J. Redmond, Adaptive template matching of photoplethysmogram pulses to detect motion artefact, Physiol. Meas. 39 (2018) 105005, https://doi.org/10.1088/1361-6579/AADF1E.
[88] S. Cherif, D. Pastor, Q.T. Nguyen, E. L'Her, Detection of artifacts on photoplethysmography signals using random distortion testing, in: Proceedings of the Annual International Conference of the IEEE Engineering in Medicine and Biology Society, EMBS 2016-October, 2016, pp. 6214–6217, https://doi.org/10.1109/EMBC.2016.7592148.